Electronic Supplementary Material (ESI) for Journal of Materials Chemistry A.


# Supplementary Information

## Synthesis of nitrogen-doped carbon nanoboxes with pore structure derived from zeolite and their excellent performance in capacitive deionization

Keyang Li [a], Shaoqing Zhu [b], Shunan Zhao [b], Ming Gong [a], Xiaohuan Zhao [a, c, d], Jie Liang [a,c], Jianning Gan [a], Yilun Huang[d, *], Ming Zhao [a], Daming Zhuang [a], Qianming Gong [a, *]

[a] Key Laboratory for Advanced Materials Processing Technology, School of Materials Science and Engineering, Tsinghua University, Beijing 100084, PR China

[b] Center for Water and Ecology, State Key Joint Laboratory of Environment Simulation and Pollution Control, School of Environment, Tsinghua University, Beijing 100084, China.

[c] School of Chemistry and Chemical Engineering, Beijing Institute of Technology, Beijing 100081, PR China

[d] SINOPEC Beijing Research Institute of Chemical Industry, Beijing 100013, PR China

[*] Corresponding authors. e-mail address: gongqianming@mail.tsinghua.edu.cn (Q. Gong).

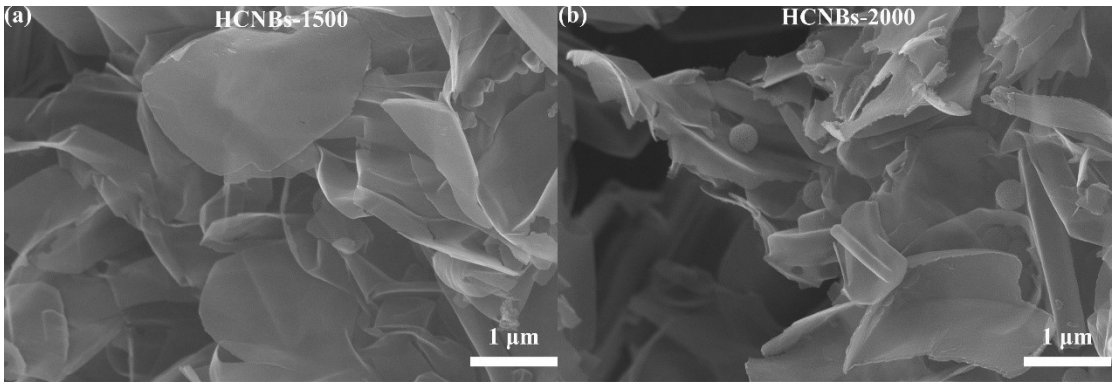


**Figure S1**: Programmed high-temperature treatment of the HCNBs-samples. The numerical postfix of the sample names was added according to the temperature of the final process in the treatment.

**Table S1** The conductivities of densely compacted HCNBs by Hall Effect Measurement System .

| Sample | HCNBs-800 | HCNBs-1000 | HCNBs-1200 |
|---|---|---|---|
| Conductivity/(S·cm$^{-1}$) | 3.43±0.12 | 4.72±0.07 | 6.25±0.09 |

**Table S2** Porous structure and nitrogen atomic percentage of the HCNBs samples carbonized at relative high temperature (1500 °C and 2000 °C).

| Sample name | Specific surface area ($m^2/g$) | Pore volume (mL/g) | Micropore volume (mL/g) | Atomic percentage of N (%) |
|---|---|---|---|---|
| HCNBs-1500 | 107.8 | 0.042 | 0.031 | 1.12 |
| HCNBs-2000 | 98.2 | 0.019 | 0.014 | 0.76 |

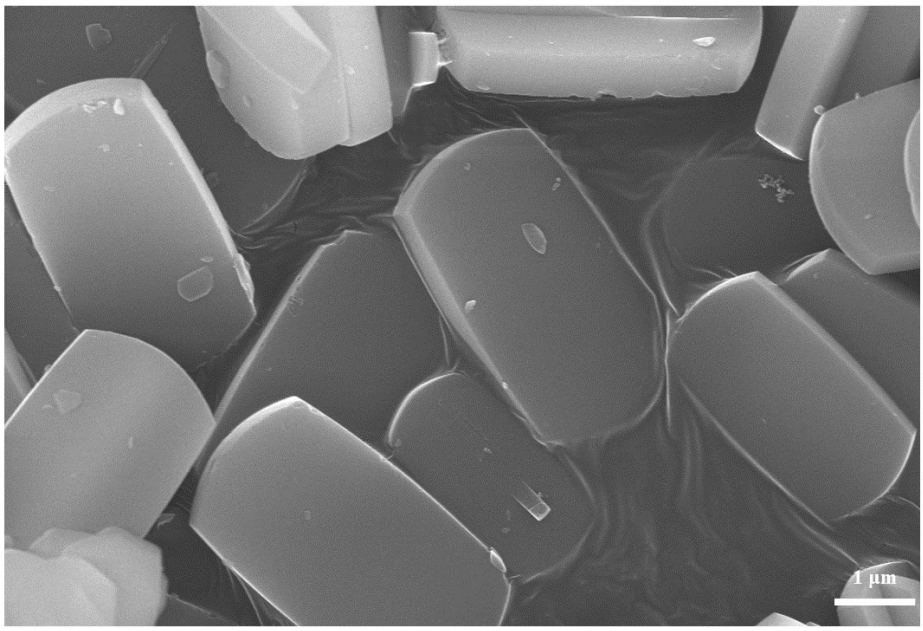


**Fig S2** SEM image of the ZSM-5 particles.

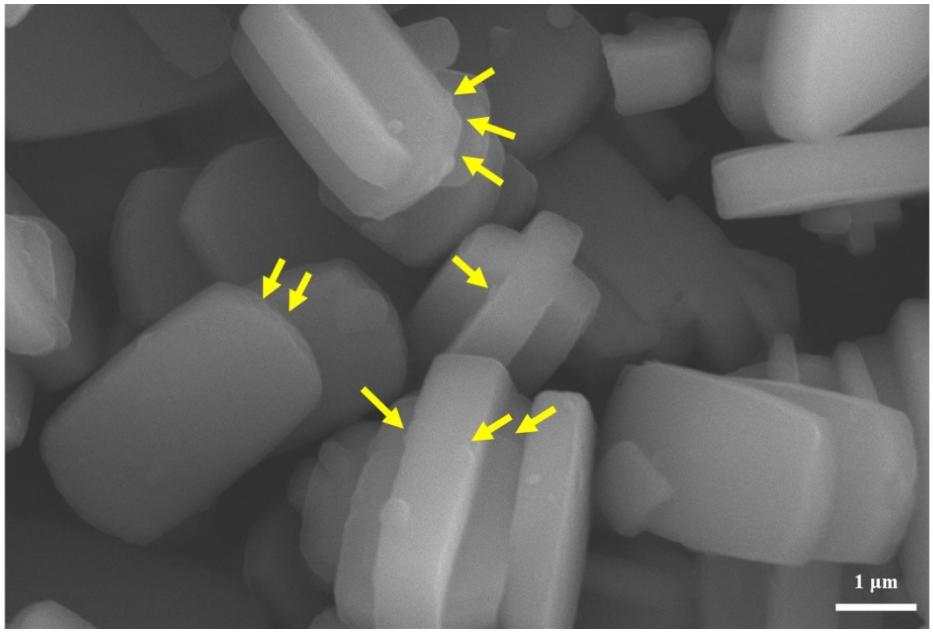


**Fig S3** SEM image of the ZSM-5 particles coated by the in-situ grown 3-aminophenol-formaldehyde resin (ZSM-5@AFP precursor). Yellow arrows are added on the image to point out the obvious polymer layers.

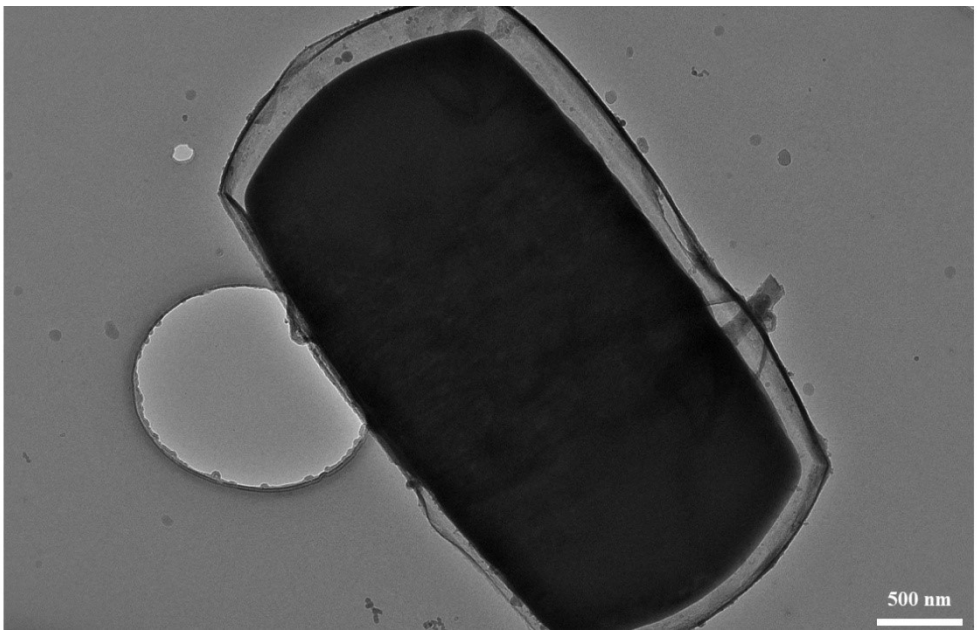


**Fig S4** TEM images of the ZSM-5 particle coated by APF derived carbon (ZSM-5@AFP carbon).

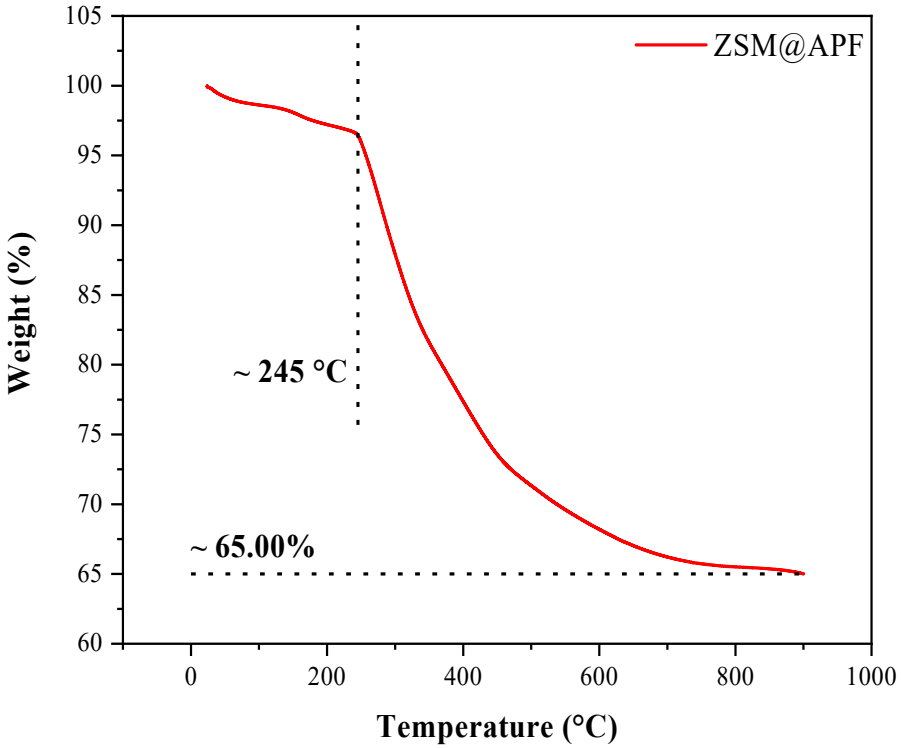


**Fig S5.** TGA analysis of ZSM@APF samples.

**Table S3** Existing forms of the doped nitrogen and oxygen atoms and their atomic percentage according to the XPS $N_{1s}$ and $O_{1s}$ spectrum.

| | HCNBs-800 | HCNBs-1000 | HCNBs-1200 |
|---|---|---|---|
| Pyridinic N (%) | 28.68 | 30.94 | 17.64 |
| Pyrrolic N (%) | 14.44 | 23.52 | 15.08 |
| Graphitic N (%) | 39.13 | 28.68 | 30.19 |
| Oxidized N (%) | 17.75 | 16.86 | 37.26 |
| Atomic percentage of N (%) | 7.11 | 6.29 | 4.92 |
| C=O (%) | 18.86 | 23.53 | 30.34 |
| C-O-O/C-OH (%) | 45.80 | 43.10 | 39.32 |
| COOH (%) | 35.34 | 33.37 | 30.36 |
| Atomic percentage of O (%) | 7.43 | 6.39 | 5.61 |

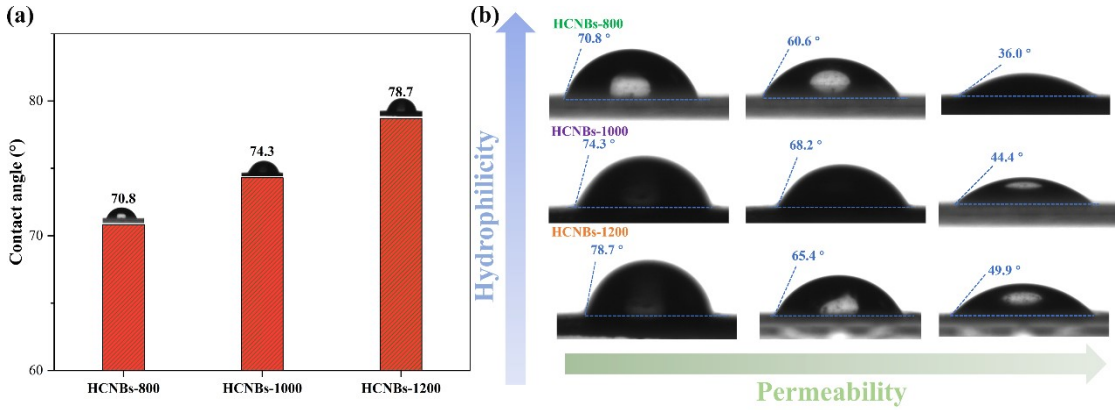


**Fig S6 (a)** Contact angle comparation results of the HCNBs samples. **(b)** Dynamic contact angle measurements of HCNBs

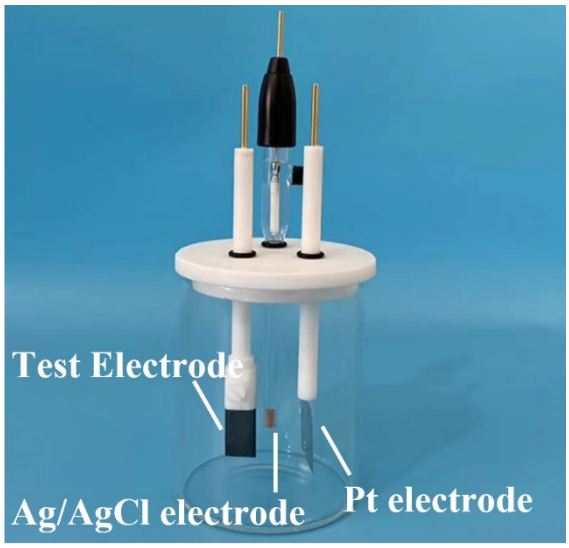


**Fig S7** Image of the three electrodes system applicated to investigate the electrochemical performance of the HCNBs-based electrodes.

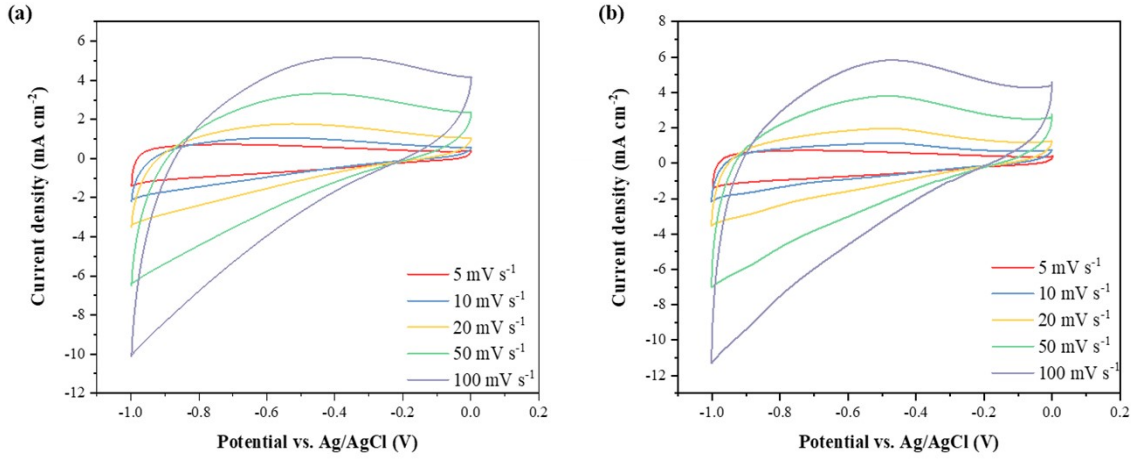


**Fig S8** CV profiles of HCNBs-800 **(a)** and HCNBs-1200 **(b)** electrodes under different scanning rate from 5 mV s-1 to 100 mV s-1 in a voltage window from -1.0 V to 0 V

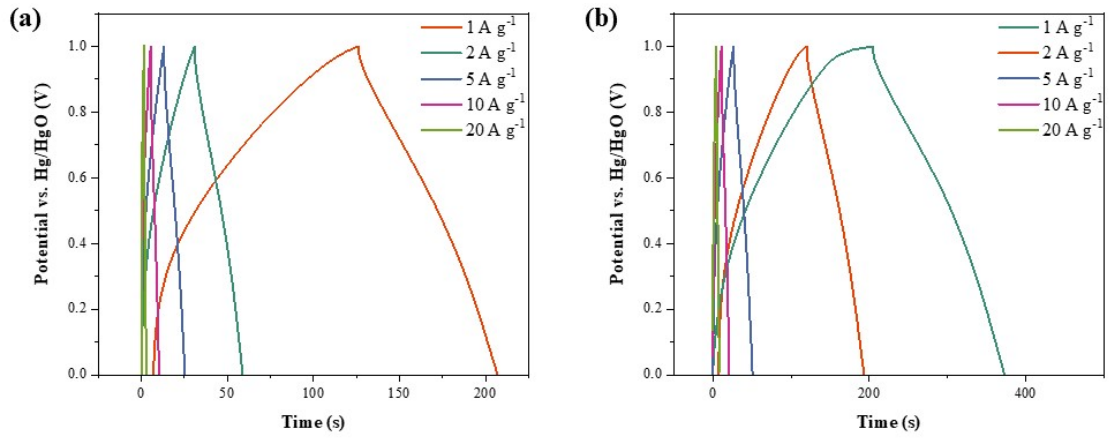


**Fig S9** GCD profiles of HCNBs-800 **(a)** and HCNBs-1200 **(b)** electrodes at different current density from 1 A·g-1 to 20 A·g-1

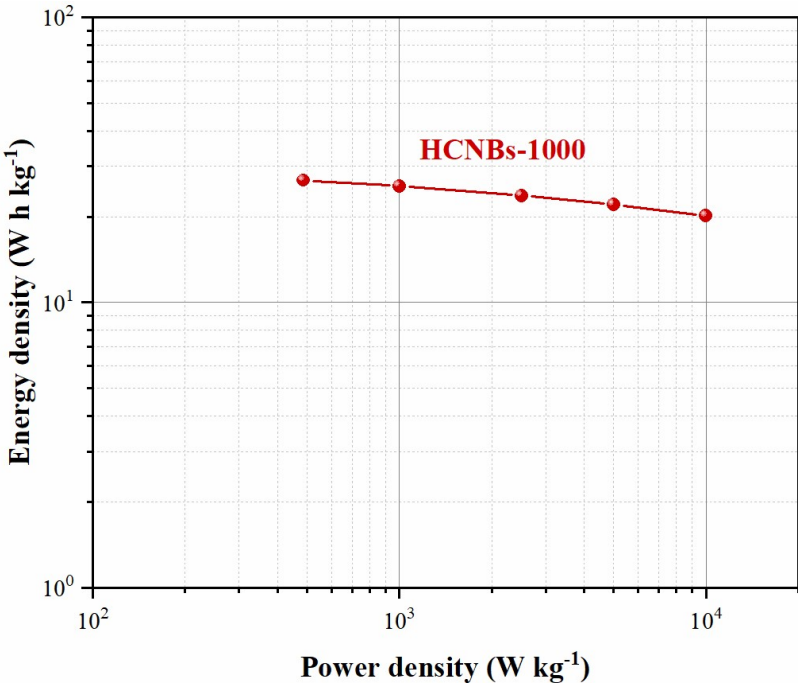


**Fig S10** Ragone plot of the HCNBs-1000-based electrodes.

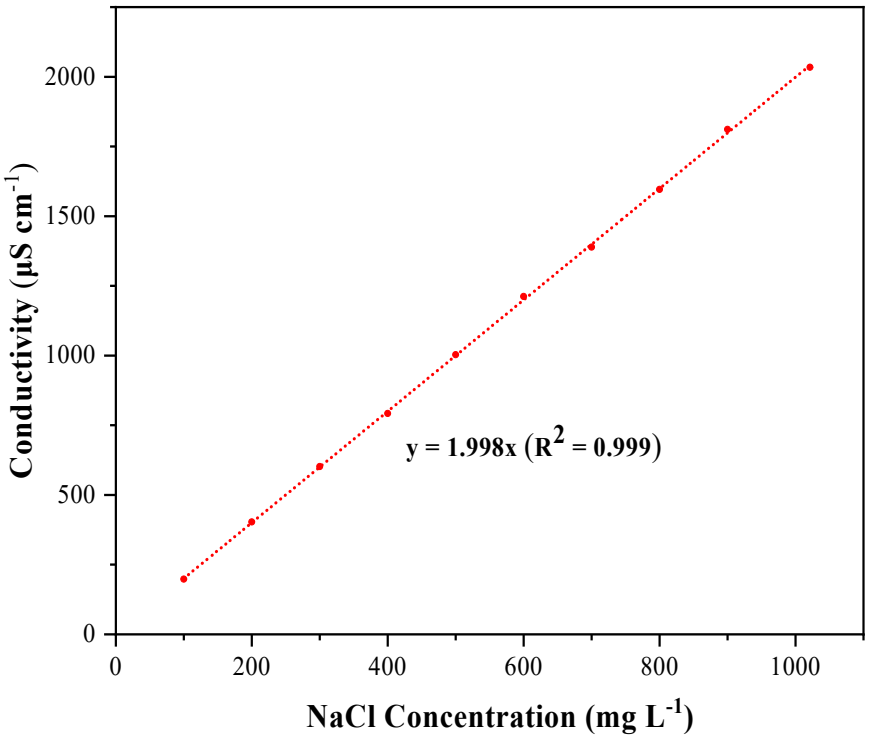


**Figure S11**: Linear correlation between NaCl concentration (mg $L^{-1}$) and solution conductivity (µS $cm^{-1}$)

**Table S4**: Desalination capacities of different carbon and carbon-based materials from the previously reported works under different voltage and NaCl concentration.

| Materials | NaCl concentration ($mg \cdot L^{-1}$) | Operation potential (V) | Desalination capacity ($mg \cdot g^{-1}$) | Ref. |
|---|---|---|---|---|
| GO/CNF webs | 450 | 1.2 | 13.2 | 1 |
| mycelium derived carbon | 500 | 1.4 | 24.17 | 2 |
| PPCP800 | 1000 | 1.2 | 14.62 | 3 |
| PCNSs | 500 | 1.1 | 15.6 | 4 |
| C-Zn | 500 | 1.5 | 16.2 | 5 |
| Mg-MOFs derived carbon | 500 | 1.2 | 16.82 | 6 |
| PDLCN | 500 | 1.2 | 18.8 | 7 |
| rGO/PC-10 | 500 | 1.2 | 25.1 | 8 |
| foamy carbon | 500 | 1.2 | 30.2 | 9 |
| P-CNF | 500 | 1.2 | 30.4 | 10 |
| NP-EHPC | 500 | 1.2 | 24.14 | 11 |
| PPD-CNTs@MC | 600 | 1.2 | 17.5 | 12 |
| **HCNBs** | **500** | **1.4** | **32.3** | **This work** |

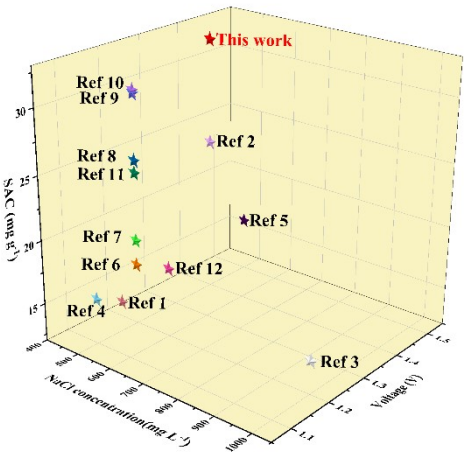


**Fig S12** Comparation of the SAC capacity of this work and previously reported carbon-based materials.

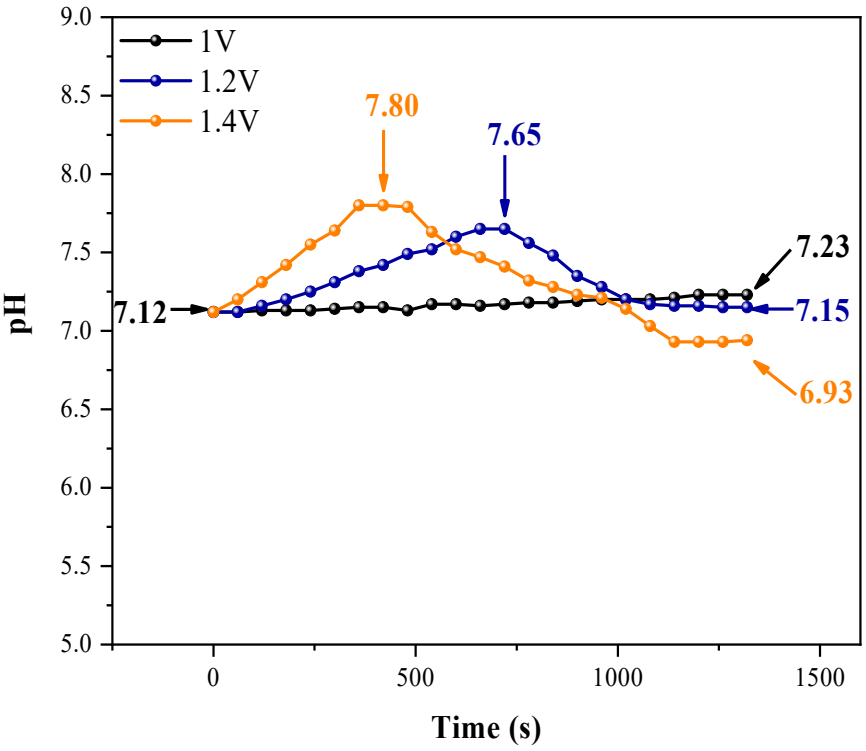


**Fig S13.** Mearsurement of pH during the desalination process under different voltage (1 V, 1.2 V and 1.4 V, HCNBs-1000-based electrodes, 500 mg·L$^{-1}$ NaCl solution)

$$O_2 + 2H_2O + 4e^- \rightarrow 4OH^-, \varphi^\theta = 0.4009\ V \#SR(1)$$

$$\begin{cases} O_2 + H_2O + 2e^- \rightarrow HO_2^- + OH^-, \varphi^\theta = -0.065\ V \\ HO_2^- + H_2O + 2e^- \rightarrow 3OH^-, \varphi^\theta = 0.867\ V \end{cases} \#SR(2)$$

$$2Cl^- \rightarrow Cl_2 + 2e^-, \varphi^\theta = 1.360\ V \#SR(3)$$

$$Cl_2 + H_2O \rightarrow HCl + HOCl \#SR(4)$$

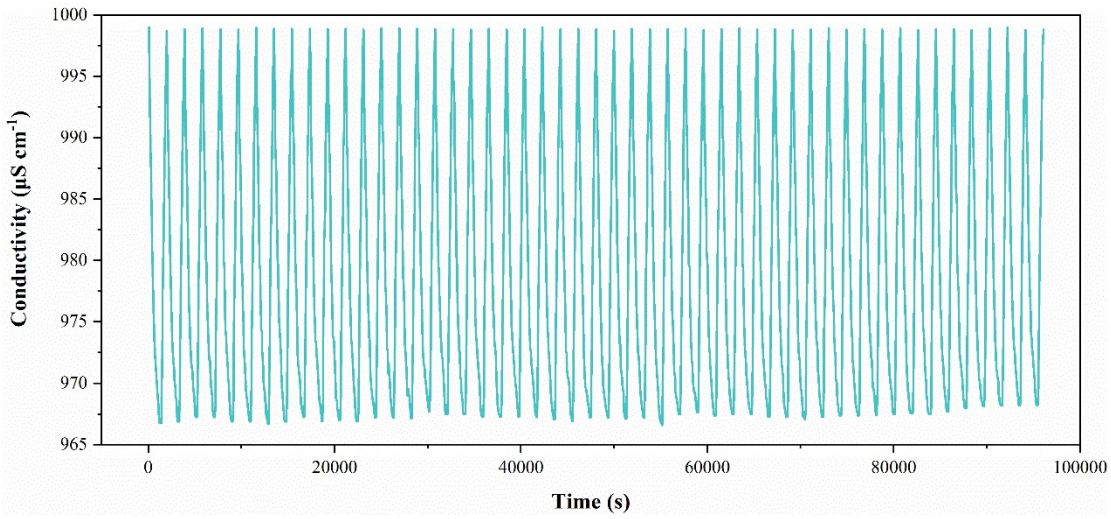


**Fig S14.** The conductivity fluctuationof NaCl solution during 50 cycles of charging/discharging for HCNBs-1000 electrodes (500 mg·$L^{-1}$, 1.4 V).

**Table S5**. Charge efficiencies of HCNBs-1000 electrode at different charging voltages with an initial NaCl concentration of 500 mg $L^{-1}$.

| Charging voltage /V | 1 | 1.2 | 1.4 |
|---|---|---|---|
| Charge efficiency | 0.703 | 0.755 | 0.812 |

**Table S6**. Charge efficiencies of HCNBs-1000 electrode at different initial NaCl concentrations at charging voltage of 1.4 V.

| Initial concentration /mg $L^{-1}$ | 125 | 250 | 500 |
|---|---|---|---|
| Charge efficiency | 0.847 | 0.826 | 0.812 |

**Reference:**


1. Y. Bai, Z. H. Huang, X. L. Yu and F. Y. Kang, *Colloids and Surfaces a-Physicochemical and Engineering Aspects*, 2014, **444**, 153-158.
2. C. Zhao, Q. Wang, S. Z. Chang, S. Zhang, Z. H. Li, Z. H. Shen, X. Jin, H. Xiao and H. G. Zhang, *Carbon*, 2022, **196**, 699-707.
3. W. L. Xing, M. Zhang, J. Liang, W. W. Tang, P. C. Li, Y. Luo, N. Tang and J. Y. Guo, *Separation and Purification Technology*, 2020, **251**.
4. T. T. Wu, G. Wang, Q. Dong, F. Zhan, X. Zhang, S. F. Li, H. Y. Qiao and J. S. Qiu, *Environmental Science & Technology*, 2017, **51**, 9244-9251.
5. Z. Z. Xie, X. H. Shang, J. B. Yan, T. Hussain, P. F. Nie and J. Y. Liu, *Electrochimica Acta*, 2018, **290**, 666-675.
6. C. P. Li, Y. Q. Wu, F. Y. Zhang, L. X. Gao, D. Q. Zhang and Z. X. An, *Separation and Purification Technology*, 2021, **277**.
7. C. P. Li, Y. Q. Wu, L. X. Gao, D. Q. Zhang and Z. X. An, *Journal of Environmental Chemical Engineering*, 2022, **10**.
8. B. F. Li, Z. H. Xiao, Y. T. Cao, Z. Q. Yu, Y. K. Sun, Z. C. Li, Y. X. Wang, Z. F. Gao and C. M. Xu, *Fuel*, 2023, **352**.
9. C. P. Li, Y. Q. Wu, J. J. An, L. X. Gao, D. Q. Zhang, J. Li and Z. X. An, *Desalination*, 2023, **559**.
10. P. F. Nie, S. P. Wang, X. H. Shang, B. Hu, M. H. Huang, J. M. Yang and J. Y. Liu, *Desalination*, 2021, **520**.
11. H. Zhang, C. H. Wang, W. X. Zhang, M. Zhang, J. W. Qi, J. S. Qian, X. Y. Sun, B. Yuliarto, J. Na, T. Park, H. G. A. Gomaa, Y. V. Kaneti, J. W. Yi, Y. Yamauchi and J. S. Li, *Journal of Materials Chemistry A*, 2021, **9**, 12807-12817.
12. Y. Lian, D. W. Wang, H. X. Guo, Z. L. Cao, J. Zhao and H. H. Zhang, *Carbon*, 2023, **204**, 50-56.